Inhibitory effects of iron depletion plus eribulin on the breast cancer microenvironment

Wataru Goto
Osaka City University Graduate School of Medicine
Shinichiro Kashiwagi (spqv9ke9@view.ocn.ne.jp)
Osaka City University Graduate School of Medicine https://orcid.org/0000-0002-0460-9599
Yuka Asano
Osaka City University Graduate School of Medicine
Koji Takada
Osaka City University Graduate School of Medicine
Tamami Morisaki
Osaka City University Graduate School of Medicine
Katsuyuki Takahashi
Osaka City University Graduate School of Medicine
Hisakazu Fujita
Osaka City University Graduate School of Nursing
Masatsune Shibutani
Osaka City University Graduate School of Medicine
Ryosuke Amano
Osaka City University Graduate School of Medicine
Tsutomu Takashima
Osaka City University Graduate School of Medicine
Shuhei Tomita
Osaka City University Graduate School of Medicine
Kosei Hirakawa
Osaka City University Graduate School of Medicine
Masaichi Ohira
Osaka City University Graduate School of Medicine

Research article

Keywords: iron, deferoxamine, eribulin mesylate, breast cancer, xenograft, epithelial-mesenchymal transition, immune checkpoints

Posted Date: March 9th, 2020

DOI: https://doi.org/10.21203/rs.3.rs-16369/v1

Version of Record: A version of this preprint was published on December 10th, 2020. See the published version at https://doi.org/10.1186/s12885-020-07673-9.

Abstract

Background Iron is required for the proliferation of cancer cells, and its depletion suppresses tumor growth. Eribulin mesylate (eribulin), a non-taxane microtubule inhibitor, disrupts the tumor microenvironment via vascular remodeling and obstruction of the epithelial-mesenchymal transition (EMT). Herein, we investigated the effects of the iron chelator deferoxamine (DFO) on tumor-related properties of breast cancer cells and the effects of DFO plus eribulin on tumor growth in vivo . Methods A triple-negative breast cancer (TNBC) cell line (MDA-MB-231) was used in our study. Cell proliferation, cell migration, cell cycle position, and gene expression were analyzed via MTT assays, wound-healing assays, flow cytometry, and quantitative real-time-polymerase chain reaction, respectively. For the in vivo experiments, mice with MDA-MB-231 xenografts were treated with the inhibitors, alone or together, and tumor volume was determined. Results DFO inhibited breast cancer cell proliferation and migration and decreased the proportion of S-phase cells. Conversely, it induced hypoxia, angiogenesis, EMT, and immune checkpoints, as determined by quantifying the expression of marker mRNAs. Eribulin suppressed the expression of the EMT marker mRNAs in the presence of DFO. DFO plus eribulin inhibited tumor growth in vivo to a greater extent than did either inhibitor alone. Conclusions Although DFO induces oncogenic events (hypoxia, angiogenesis, EMT, and immune checkpoints), it may be an effective treatment for breast cancer when administered in combination with eribulin.

Background

Iron is an essential requirement for both normal and cancer cell viability and proliferation. The protein transferrin shuttles iron from the serum to the cell interior via transferrin receptor 1 (TfR1) [1]. Cancer cells have significantly higher levels of TfR1 than do normal cells and hence take up iron more rapidly [2]. Iron has been shown to increase the expression of cyclin D1, D2, and D3, which facilitates G1/S cell cycle progression [3], and is distributed in the hemoglobin of red blood cells, where it promotes oxygen transport. Conversely, iron depletion inhibits cyclin D1 expression [3, 4], suppresses tumor growth [5], and reduces serum hemoglobin levels and oxygen supply to tissues [6, 7]. These observations implicate iron in tumor progression; however, the effect of iron on the epithelial-mesenchymal transition (EMT) or immune checkpoints has not been examined sufficiently.

Eribulin mesylate (eribulin), a non-taxane, synthetic inhibitor of microtubule dynamics, induces G2/M cell cycle arrest and subsequent apoptosis [8–10]. Interestingly, it also has some unique anticancer effects in breast cancer cells, such as improvement of tumor perfusion, hypoxia [11], and the EMT [12]. We previously investigated these effects using clinical tumor samples [13] and suggested that eribulin enhanced the antitumor immune response by inactivating immune checkpoints [14]. The present study investigated the mechanism of iron control therapy in breast cancer in terms of the tumor microenvironment. We also determined whether the combination of iron depletion and eribulin was a potentially effective treatment for breast cancer.

Methods

Cell lines and culture conditions

MDA-MB-231 (ATCC HTB-26), a triple-negative breast cancer (TNBC) cell line, was purchased from the American Type Culture Collection (Rockville, MD, USA). Cells were cultured in Dulbecco's Modified Eagle's Medium (DMEM; Wako, Osaka, Japan) supplemented with 10% fetal bovine serum (FBS; Equitech-Bio, Kerrville, TX, USA), 100 µg/mL streptomycin, and 100 U/mL penicillin (Gibco, Grand Island, NE, USA) at 37 °C in a humidified chamber with 5% CO_2. The culture medium was replaced every 3 days.

Compounds

Deferoxamine (DFO), an iron-chelating agent, was purchased from Novartis (Basel, Switzerland). Eribulin was provided by Eisai Co. (Tokyo, Japan).

Cytotoxicity assay

The sensitivity of the three human breast cancer cell lines to DFO was evaluated using a cell proliferation (MTT) assay kit according to the manufacturer's instructions (Sigma-Aldrich, St. Louis, MO, USA). Briefly, cells (1×10^3 cells/well in 96-well plates) were cultured for 24 h in 90 µL of DMEM with 10% FBS. A 10-µL aliquot of medium containing the indicated concentration of DFO was then added to each well. After incubation for 72 h, 10 µL of the MTT reagent was added to each well; 2 h later, the medium was discarded and replaced by 100 µL of dimethyl sulfoxide. After shaking the plates for 10 min, the absorbance of each well was measured at 510 nm using a microplate reader (Perkin-Elmer, Waltham, MA, USA). All samples were analyzed at least three times.

Wound-healing assay

MDA-MB-231 cells were cultured in 96-well plates. After the cells reached 80–90% confluence, a wound was created in the cell monolayer using the WoundMaker tool (Essen Bioscience, Ann Arbor, MI, USA). The cells were cultured in DMEM with 5% FBS and 10 or 100 µM DFO for 30 h. Scratched fields were photographed every 3 h using an Incucyte Live-Cell Imaging System (Essen Bioscience). The degree of cell migration was calculated as 100 × the wound closure area at each time point/the wound area at time 0.

Analysis of cell cycle progression

Cells (1×10^6 cells/well) were seeded into six-well tissue culture plates. After 24 h, the cells were harvested and washed twice with phosphate-buffered saline and stained using the CycleTEST™ PLUS DNA Reagent kit according to the manufacturer's instructions (Becton Dickinson Biosciences, CA-San Jose, USA). Staining intensity was quantified using a BD LSR II flow cytometer with FACSDiva™ software (Becton Dickinson Biosciences).

Quantitative real-time-polymerase chain reaction (qRT-PCR)

Total RNA was extracted from cells using a RNeasy Mini kit (Qiagen, Valencia, CA, USA). cDNA was amplified via qRT-PCR using Taq DNA polymerase (Nippon Gene, Tokyo, Japan) and the StepOnePlus RT-

PCR system (Applied Biosystems, Foster City, CA, USA). The following TaqMan gene expression assays for used: assay ID, Hs00154208 (CA9); assay ID, Hs00911700 (KDR); assay ID, Hs00983056 (CDH2); assay ID, Hs01125301 (CD274); and assay ID, Hs02758991 (GAPHD) (Applied Biosystems). RT-PCR was performed at 95 °C for 15 s, followed by 40 cycles at 60 °C for 60 s.

In vivo tumor model

In vivo experiments were conducted on 4-week-old female athymic BALB/c nu/nu mice (CLEA Japan, Tokyo, Japan) using a protocol approved by the Osaka City University Ethical Committee, Osaka, Japan. All studies on mice were conducted in accordance with the National Institute of Health (NIH) 'Guide for the Care and Use of Laboratory Animals'. The mice were housed in a standard animal laboratory with ad libitum access to food and water. MDA-MB-231 cells (10^7 cells) were injected into the backs of the mice to produce subcutaneous xenografts. After a week, the mice were randomized into two groups: (1) control and (2) DFO (20 mg/kg/day, 5 days/week). For evaluation of the combination therapy, the mice were randomized into four groups: (1) control, (2) DFO alone, (3) eribulin alone (0.8 mg/kg/day, 5 days/week), and (4) DFO plus eribulin. DFO was directly injected into the tumor, and eribulin was intravenously administered. The volumes (length × width) of the resultant tumors were measured weekly. Animals were sacrificed and autopsied at 6 weeks after cell inoculation.

Statistical analysis

Statistical analyses were performed using JMP13 software (SAS Institute, Cary, NC, USA). Comparisons between groups were made using Student's t-test. A p value < 0.05 was considered to indicate statistical significance.

Results

Effects of DFO on breast cancer cell proliferation and migration

DFO suppressed the proliferation of MDA-MB-231 cells in a dose-dependent manner in MTT assays (Fig. 1a). It also inhibited the migration of MDA-MB 231 cells in wound-healing assays at 100 μM and suppressed ($p = 0.027$) (Fig. 1b) tumor growth in nude mice with subcutaneous MDA-MB-231 xenographs (tumor volume: control vs. iron-deficient = 159.9 ± 14.7 mm² vs. 58.5 ± 12.1 mm²; $p < 0.001$) (Fig. 1c). No significant side effects were observed in DFO-treated mice. As shown via flow cytometry, DFO reduced the proportion of MDA-MB-231 cells in S phase (Fig. 2). This finding suggests that iron depletion inhibits the G1/S transition.

Effects of DFO on mRNA expression in breast cancer cells

In these experiments, cells were treated with or without DFO for 3 days. Total RNA was extracted, and the expression levels of the indicated mRNAs were quantified via qRT-PCR.

The effects of iron depletion on hypoxia and angiogenesis were examined by measuring the mRNA levels of CA9 and KDR, respectively. CA9 encodes carbonic anhydrase 9, which is overexpressed in hypoxic conditions, and KDR encodes vascular endothelial growth factor receptor 2, which promotes angiogenesis. Notably, DFO upregulated CA9 expression in MDA-MB-231 cells, indicating that iron deficiency induces hypoxia ($p = 0.0378$) (Fig. 3a). It also slightly increased the mRNA levels of KDR in MDA-MB-231 (Fig. 3b).

The effects of iron deficiency on the EMT and immune checkpoints were assessed by measuring the mRNA levels of CDH2 and CD274, respectively. CDH2 encodes N-cadherin, which is expressed by mesenchymal cells, and CD274 encodes programmed death-ligand 1 (PD-L1), which activates an immune checkpoint. CDH2 expression levels were higher in DFO-treated MDA-MB-231 cells than in untreated cells (Fig. 3c), as were CD274 expression levels (Fig. 3d).

Effects of eribulin plus DFO on tumor growth in mice

Our data suggest that DFO has both anti-oncogenic (inhibition of proliferation and migration) and oncogenic (induction of hypoxia, EMT, and immune checkpoints) effects. Because we have shown that eribulin blocks these oncogenic events [13, 14], we asked whether DFO might more effectively suppress tumor growth in the presence of eribulin. Eribulin reduced CDH2 expression in the presence of DFO ($p = 0.0174$) (Fig. 4a). Hence, eribulin apparently antagonizes the induction of hypoxia, EMT, and immune checkpoints by iron depletion in breast cancer cells. Importantly, DFO plus eribulin inhibited the growth of MDA-MB-231 xenografts in nude mice to a greater extent than did either agent alone (tumor volume: control [270.0 ± 35.7 mm^2], iron-deficient [203.5 ± 33.2 mm^2], eribulin [141.9 ± 15.1 mm^2], iron-deficient + eribulin [96.3 ± 13.8 mm^2]) ($p = 0.0181$, $p = 0.0067$, $p = 0.0060$, respectively) (Fig. 4b).

Discussion

In the present study, the iron chelator DFO suppressed breast cancer cell proliferation, migration, and tumor growth, but induced angiogenesis, hypoxia, EMT, and immune checkpoints. Regarding mechanism, we suggest that DFO promotes angiogenesis via hypoxia. To the best of our knowledge, our study is the first to examine the effects of iron depletion on the tumor immune microenvironment. Our model whereby DFO elicits its various effects is presented in Fig. 5.

As shown in a previous study, DFO induces hypoxia and the consequent expression of hypoxia-inducible factor-1 alpha (HIF-1α) in breast cancer cells [15]. HIF-1α initiates the transcription of genes encoding angiogenesis-promoting proteins such as vascular endothelial growth factor [16]. It also increases TfR expression, stimulates iron uptake [2], and interacts with and stabilizes the tumor suppressor p53 [17, 18]. Once accumulated, p53 may induce G1/S arrest and apoptosis via its downstream effectors [19].

Although several factors promote the EMT via complex pathways, HIF-1α is considered to be one of the most important [20]; it upregulates two EMT inducers, Snail and TWIST1 [21]. Hypoxia-induced HIFα has also been linked to immune checkpoint activation: in a previous study, it increased the expression of PD-

L1 in myeloid-derived suppressor cells [22]. Furthermore, as shown by Noman et al., PD-L1 expression is upregulated in EMT-activated breast cancer cells, a process driven by various EMT transcription factors, including ZEB-1 and miR200 [23]. Based on these findings, we suggest that iron depletion induces the EMT and immune checkpoints via HIF-1α.

Because it elicits oncogenic events (hypoxia, EMT, and immune checkpoints), as well as anti-oncogenic events (G1/S arrest and apoptosis), iron depletion monotherapy is considered insufficient for the treatment of breast cancer. Hence, recent studies assessed the effectiveness of iron depletion plus chemotherapy. Hoke et al. found that the combination of DFO as an antioxidant and doxorubicin improved the outcomes of breast cancer patients, perhaps by reducing the toxicity of doxorubicin to cardiomyocytes and tumor growth [24]. Moreover, Ohara et al. reported that the combination of iron depletion and bevacizumab, an antiangiogenic drug, had dramatic synergistic antitumor effects [25].

Eribulin is currently an approved treatment for patients with locally advanced or metastatic breast cancer. In a phase trial (study 305/EMBRACE), eribulin significantly improved the overall survival of metastatic breast cancer patients who had previously undergone chemotherapy with anti-cancer agents such as anthracycline and taxane [26]. Since recent studies indicate that eribulin inhibits tumor hypoxia, EMT, and immune checkpoints [11–14], we hypothesized that iron depletion plus eribulin might be a useful therapy for breast cancer. No previous studies have investigated this combination therapy in breast cancer.

We found that the combination of DFO and eribulin had a significant antitumor effect in vivo compared with either inhibitor alone. Additionally, our qRT-PCR results suggest that eribulin suppressed the induction of hypoxia, EMT, and immune checkpoints by DFO in TNBC cells. We previously used tumor-infiltrating lymphocytes to monitor the tumor immune microenvironment and propose that doing so is a valid means for evaluating the therapeutic effects of eribulin in TNBC cases [27]. Our present study suggests that eribulin might act synergistically with DFO to suppress tumor growth in activated tumor immune microenvironments, such as those produced by DFO. Hence, eribulin plus iron depletion potentially represents a novel and practical treatment for breast cancer. However, eribulin incompletely suppressed the expression of the marker mRNAs for hypoxia, EMT, and immune checkpoints in DFO-treated cells (i.e., expression levels were higher in cells receiving eribulin plus DFO than in those receiving eribulin alone). Consequently, the effect of the combination on tumor suppression may be additive, not synergistic. Further studies are necessary to decipher the complex mechanisms underlying the effects of eribulin and DFO on tumor suppression and to design strategies for DFO and eribulin cotreatment of breast cancer patients in the clinical setting.

Conclusions

Iron depletion inhibits the proliferation, migration, and in vivo growth of breast cancer cells. Conversely, it induces hypoxia, EMT, and immune checkpoints, thus creating an environment conducive for tumor growth. The combination of DFO and eribulin may be an effective treatment for breast cancer.

List Of Abbreviations

DFO, deferoxamine

DMEM, Dulbecco's modified Eagle's medium

EMT, epithelial-mesenchymal transition

FBS, fetal bovine serum

NIH, National Institute of Health

PD-L1, programmed death-ligand 1

qRT-PCR, quantitative real-time-polymerase chain reaction

TfR1, transferrin receptor 1

TNBC, triple-negative breast cancer

Declarations

Ethics approval and consent to participate

Mice experiments were conducted in accordance with NIH guidelines for the care and use of laboratory animals and approved by the Osaka City University Institutional Animal Care and Use Committee. This study did not involve human participants, human data or human tissue. Mammalian cell lines used in this study do not require ethics approval.

Consent for publication

Not applicable.

Availability of data and materials

The datasets supporting the conclusions of this article is included within the article.

Competing interests

The authors declare that they have no competing interests.

Funding

This study was funded by grants from the Japan Society for the Promotion of Science (KAKENHI**,** Nos. 19K18046, 26461957, and 17K10559) to Shinichiro Kashiwagi.

Authors' contributions

All authors were involved in the preparation of this manuscript. WG collected the data, and wrote the manuscript. SK, YA, KTakada, TM, KTakahashi and TT performed the operation and designed the study. WG, SK, MS, RA and ST summarized the data and revised the manuscript. HF, KH and MO substantial contribution to the study design, performed the operation, and revised the manuscript. All authors read and approved the final manuscript.

Acknowledgements

We thank Yayoi Matsukiyo and Tomomi Okawa (Department of Surgical Oncology, Osaka City University Graduate School of Medicine) for helpful advice regarding data management.

Authors' information

[1]Department of Breast and Endocrine Surgery, Osaka City University Graduate School of Medicine, 1-4-3 Asahi-machi, Abeno-ku, Osaka 545-8585, Japan.

[2]Department of Pharmacology, Osaka City University Graduate School of Medicine, 1-4-3 Asahi-machi, Abeno-ku, Osaka 545-8585, Japan.

[3]Department of Scientific and Linguistic Fundamentals of Nursing, Osaka City University Graduate School of Nursing, 1-5-17 Asahi-machi, Abeno-ku, Osaka 545-0051, Japan.

[4]Department of Gastrointestinal Surgery, Osaka City University Graduate School of Medicine, 1-4-3 Asahi-machi, Abeno-ku, Osaka 545-8585, Japan.

[5]Department of Hepato-Biliary-Pancreatic Surgery, Osaka City University Graduate School of Medicine, 1-4-3 Asahi-machi, Abeno-ku, Osaka 545-8585, Japan.

References

1. Wang J, Pantopoulos K: Regulation of cellular iron metabolism. *Biochem J* 2011, 434(3):365-381.
2. Le NT, Richardson DR: The role of iron in cell cycle progression and the proliferation of neoplastic cells. *Biochim Biophys Acta* 2002, 1603(1):31-46.
3. Gao J, Richardson DR: The potential of iron chelators of the pyridoxal isonicotinoyl hydrazone class as effective antiproliferative agents, IV: The mechanisms involved in inhibiting cell-cycle progression. *Blood* 2001, 98(3):842-850.
4. Nurtjahja-Tjendraputra E, Fu D, Phang JM, Richardson DR: Iron chelation regulates cyclin D1 expression via the proteasome: a link to iron deficiency-mediated growth suppression. *Blood* 2007, 109(9):4045-4054.

5. Hann HW, Stahlhut MW, Blumberg BS: Iron nutrition and tumor growth: decreased tumor growth in iron-deficient mice. *Cancer Res* 1988, 48(15):4168-4170.
6. Vaupel P, Mayer A, Briest S, Hockel M: Oxygenation gain factor: a novel parameter characterizing the association between hemoglobin level and the oxygenation status of breast cancers. *Cancer Res* 2003, 63(22):7634-7637.
7. Kato J, Miyanishi K, Kobune M, Nakamura T, Takada K, Takimoto R, Kawano Y, Takahashi S, Takahashi M, Sato Y *et al*: Long-term phlebotomy with low-iron diet therapy lowers risk of development of hepatocellular carcinoma from chronic hepatitis C. *J Gastroenterol* 2007, 42(10):830-836.
8. Towle MJ, Salvato KA, Budrow J, Wels BF, Kuznetsov G, Aalfs KK, Welsh S, Zheng W, Seletsky BM, Palme MH *et al*: In vitro and in vivo anticancer activities of synthetic macrocyclic ketone analogues of halichondrin B. *Cancer Res* 2001, 61(3):1013-1021.
9. Kuznetsov G, Towle MJ, Cheng H, Kawamura T, TenDyke K, Liu D, Kishi Y, Yu MJ, Littlefield BA: Induction of morphological and biochemical apoptosis following prolonged mitotic blockage by halichondrin B macrocyclic ketone analog E7389. *Cancer Res* 2004, 64(16):5760-5766.
10. Jordan MA, Kamath K, Manna T, Okouneva T, Miller HP, Davis C, Littlefield BA, Wilson L: The primary antimitotic mechanism of action of the synthetic halichondrin E7389 is suppression of microtubule growth. *Mol Cancer Ther* 2005, 4(7):1086-1095.
11. Funahashi Y, Okamoto K, Adachi Y, Semba T, Uesugi M, Ozawa Y, Tohyama O, Uehara T, Kimura T, Watanabe H *et al*: Eribulin mesylate reduces tumor microenvironment abnormality by vascular remodeling in preclinical human breast cancer models. *Cancer Sci* 2014, 105(10):1334-1342.
12. Yoshida T, Ozawa Y, Kimura T, Sato Y, Kuznetsov G, Xu S, Uesugi M, Agoulnik S, Taylor N, Funahashi Y *et al*: Eribulin mesilate suppresses experimental metastasis of breast cancer cells by reversing phenotype from epithelial-mesenchymal transition (EMT) to mesenchymal-epithelial transition (MET) states. *Br J Cancer* 2014, 110(6):1497-1505.
13. Kashiwagi S, Asano Y, Goto W, Takada K, Takahashi K, Hatano T, Tanaka S, Takashima T, Tomita S, Motomura H *et al*: Mesenchymal-epithelial Transition and Tumor Vascular Remodeling in Eribulin Chemotherapy for Breast Cancer. *Anticancer Res* 2018, 38(1):401-410.
14. Goto W, Kashiwagi S, Asano Y, Takada K, Morisaki T, Fujita H, Takashima T, Ohsawa M, Hirakawa K, Ohira M: Eribulin Promotes Antitumor Immune Responses in Patients with Locally Advanced or Metastatic Breast Cancer. *Anticancer Res* 2018, 38(5):2929-2938.
15. Liu Y, Cui Y, Shi M, Zhang Q, Wang Q, Chen X: Deferoxamine promotes MDA-MB-231 cell migration and invasion through increased ROS-dependent HIF-1alpha accumulation. *Cell Physiol Biochem* 2014, 33(4):1036-1046.
16. Beerepoot LV, Shima DT, Kuroki M, Yeo KT, Voest EE: Up-regulation of vascular endothelial growth factor production by iron chelators. *Cancer Res* 1996, 56(16):3747-3751.
17. Fukuchi K, Tomoyasu S, Watanabe H, Kaetsu S, Tsuruoka N, Gomi K: Iron deprivation results in an increase in p53 expression. *Biol Chem Hoppe Seyler* 1995, 376(10):627-630.

18. An WG, Kanekal M, Simon MC, Maltepe E, Blagosklonny MV, Neckers LM: Stabilization of wild-type p53 by hypoxia-inducible factor 1alpha. *Nature* 1998, 392(6674):405-408.
19. Carmeliet P, Dor Y, Herbert JM, Fukumura D, Brusselmans K, Dewerchin M, Neeman M, Bono F, Abramovitch R, Maxwell P *et al*: Role of HIF-1alpha in hypoxia-mediated apoptosis, cell proliferation and tumour angiogenesis. *Nature* 1998, 394(6692):485-490.
20. Jing Y, Han Z, Zhang S, Liu Y, Wei L: Epithelial-Mesenchymal Transition in tumor microenvironment. *Cell Biosci* 2011, 1:29.
21. Cho KH, Yu SL, Cho DY, Park CG, Lee HY: Breast cancer metastasis suppressor 1 (BRMS1) attenuates TGF-beta1-induced breast cancer cell aggressiveness through downregulating HIF-1alpha expression. *BMC Cancer* 2015, 15:829.
22. Noman MZ, Desantis G, Janji B, Hasmim M, Karray S, Dessen P, Bronte V, Chouaib S: PD-L1 is a novel direct target of HIF-1alpha, and its blockade under hypoxia enhanced MDSC-mediated T cell activation. *J Exp Med* 2014, 211(5):781-790.
23. Noman MZ, Janji B, Abdou A, Hasmim M, Terry S, Tan TZ, Mami-Chouaib F, Thiery JP, Chouaib S: The immune checkpoint ligand PD-L1 is upregulated in EMT-activated human breast cancer cells by a mechanism involving ZEB-1 and miR-200. *Oncoimmunology* 2017, 6(1):e1263412.
24. Hoke EM, Maylock CA, Shacter E: Desferal inhibits breast tumor growth and does not interfere with the tumoricidal activity of doxorubicin. *Free Radic Biol Med* 2005, 39(3):403-411.
25. Ohara T, Noma K, Urano S, Watanabe S, Nishitani S, Tomono Y, Kimura F, Kagawa S, Shirakawa Y, Fujiwara T: A novel synergistic effect of iron depletion on antiangiogenic cancer therapy. *Int J Cancer* 2013, 132(11):2705-2713.
26. Cortes J, O'Shaughnessy J, Loesch D, Blum JL, Vahdat LT, Petrakova K, Chollet P, Manikas A, Dieras V, Delozier T *et al*: Eribulin monotherapy versus treatment of physician's choice in patients with metastatic breast cancer (EMBRACE): a phase 3 open-label randomised study. *Lancet* 2011, 377(9769):914-923.
27. Kashiwagi S, Asano Y, Goto W, Takada K, Takahashi K, Noda S, Takashima T, Onoda N, Tomita S, Ohsawa M *et al*: Use of Tumor-infiltrating lymphocytes (TILs) to predict the treatment response to eribulin chemotherapy in breast cancer. *PLoS One* 2017, 12(2):e0170634.

Figures

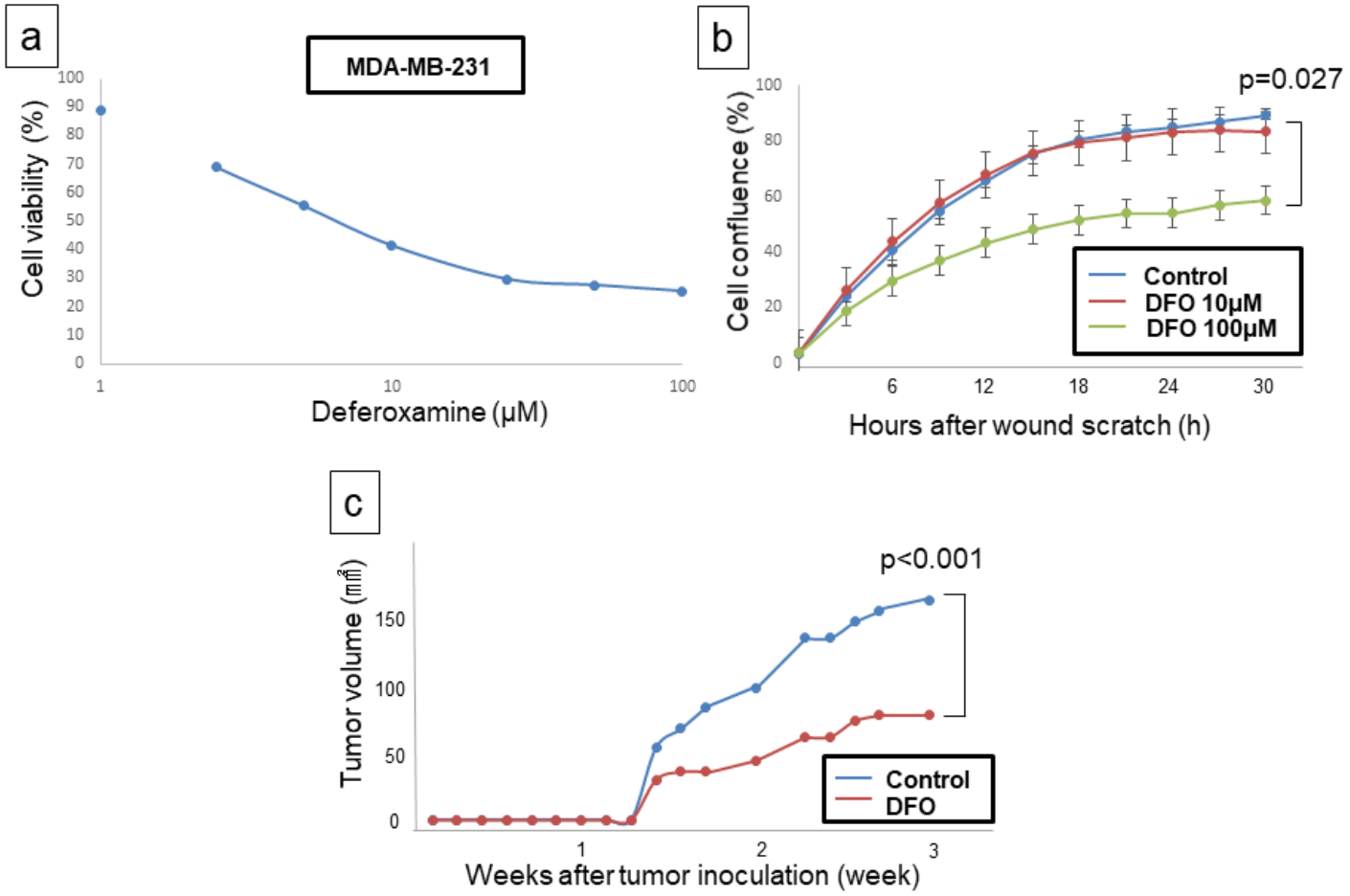

Figure 1

Cytotoxicity of deferoxamine (A). The sensitivity of MDA-MB-231 cell lines to deferoxamine was evaluated via an MTT assay. Deferoxamine suppressed cell proliferation of breast cancer cells in a dose-dependent manner. Effect of deferoxamine on the migration of breast cancer cells (p = 0.027) (B). The proportion of MDA-MB-231 cells migrating across the wound was decreased by deferoxamine administration compared with the control. Tumor volumes of MDA-MB-231 cells xenograft in the group of control and deferoxamine administration in mice (tumor volume: control vs. iron-deficient = 159.9 ± 14.7 mm^2 vs. 58.5 ± 12.1 mm^2; p < 0.001) (C). The results of this analysis showed that the size of MDA-MB-231xenografts in the iron-deficient group was smaller than those in control group.

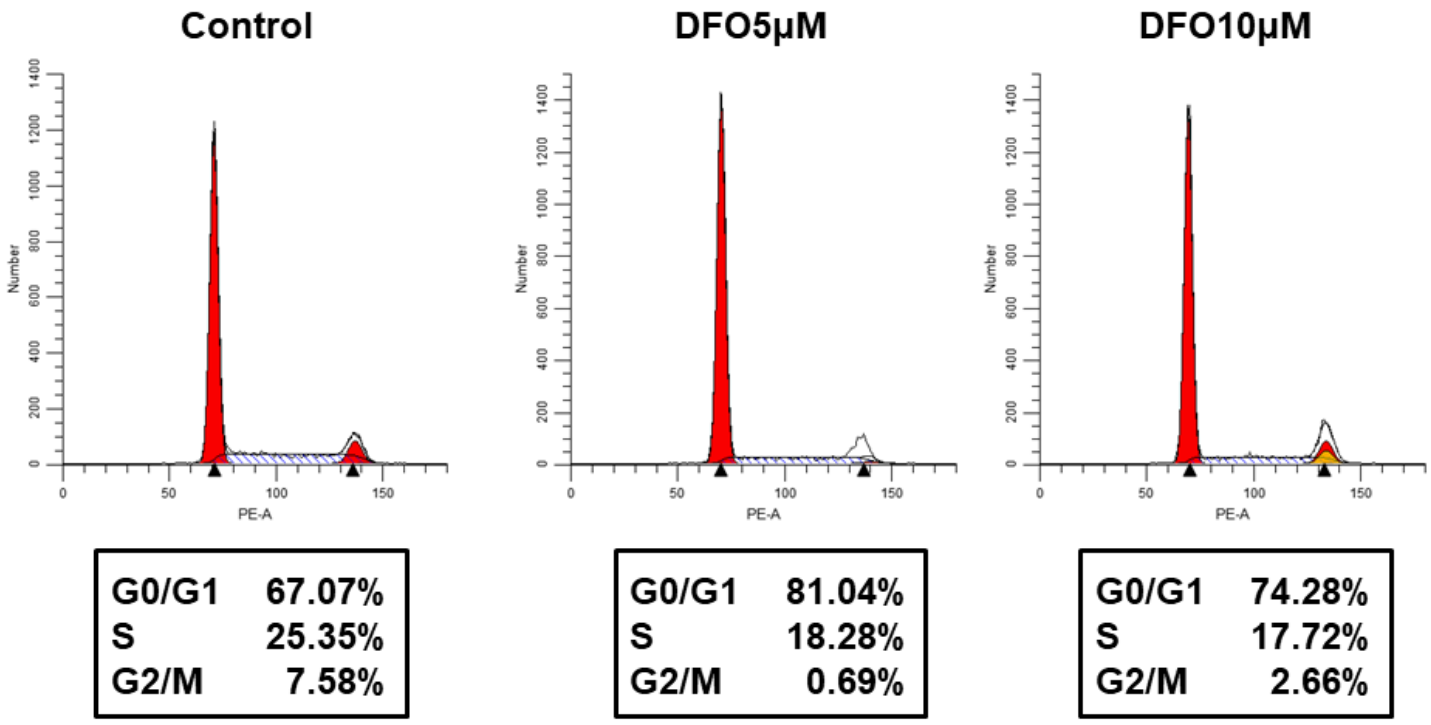

Figure 2

Cell cycle analysis of MDA-MB-231 and MDA-MB-231+deferoxamine. The results of this analysis showed that the proportion of MDA-MB-231 cells that were in G0/G1 was decreased, after deferoxamine treatment.

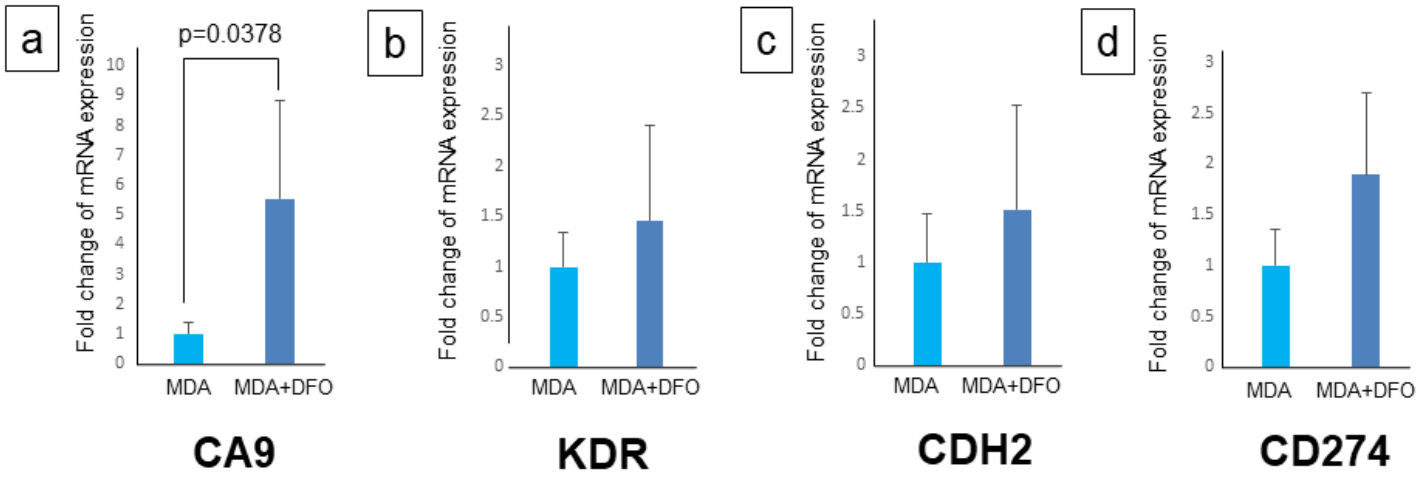

Figure 3

Expression levels of CA9 related gene in deferoxamine-treated MDA-MB-231 cells as measured by RT-PCR (A). DFO upregulated CA9 expression in both MDA-MB-231 cells, indicating that iron deficiency induces hypoxia (p = 0.0378). Expression levels of VEGFR2 related gene in deferoxamine-treated MDA-MB-231 cells as measured by RT-PCR (B). Deferoxamine treatment increased KDR expression levels in MDA-MB-231 cells. Expression levels of N-cadherin related gene in deferoxamine-treated MDA-MB-231 cells as measured by RT-PCR (C). Deferoxamine treatment increased CDH2 expression levels in MDA-MB-231 cells. Expression levels of PD-L1 related gene in deferoxamine-treated MDA-MB-231 cells as measured by RT-PCR (D). Deferoxamine treatment increased CD274 expression levels in MDA-MB-231 cells.

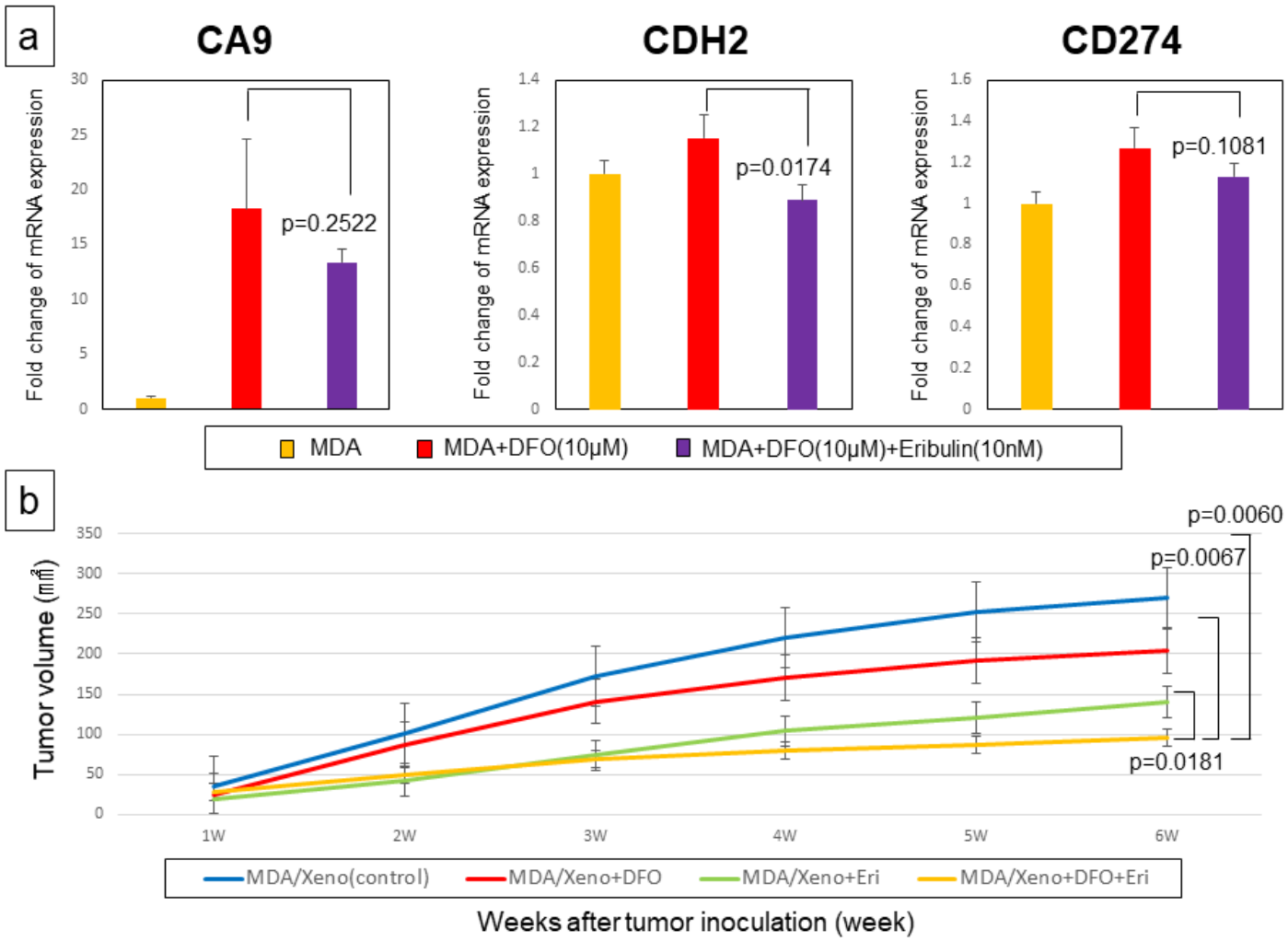

Figure 4

Expression levels of CA9, N-cadherin and PD-L1 related gene in MDA-MB-231 cells treated with combination therapy of eribulin and deferoxamine as measured by RT-PCR (A). Eribulin downregulated CDH2 expression levels in iron-deficient MDA-MB-231 cells by treated with deferoxamine ($p = 0.0174$). However, the mRNA expression in the group of combination therapy were not suppressed compared to the group of eribulin alone. Tumor volumes of MDA-MB-231 cells xenograft in the group of control, deferoxamine alone, eriublin alone and combination of eribulin and deferoxamine in mice (tumor volume: control [270.0 ± 35.7 mm^2], iron-deficient [203.5 ± 33.2 mm^2], eribulin [141.9 ± 15.1 mm^2], iron-deficient + eribulin [96.3 ± 13.8 mm^2]) ($p = 0.0181$, $p = 0.0067$, $p = 0.0060$, respectively) (B). The results of this analysis showed that tumor growth of MDA-MB-231cells xenografts in the combination treatment group was inhibited compared to eribulin alone or deferoxamine alone group.

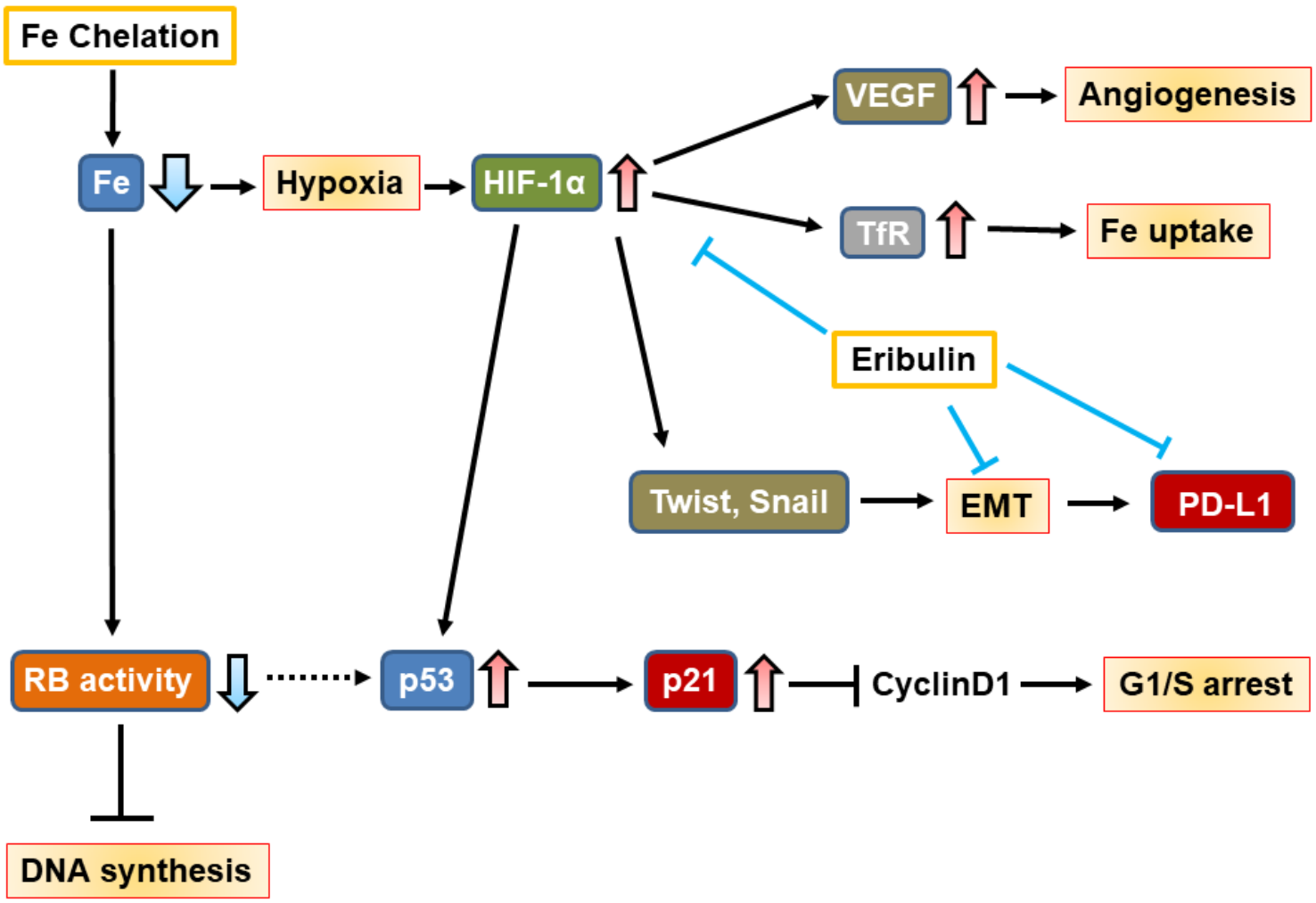

Figure 5

Schematic illustration of the effects of iron chelation and eribulin. Iron depletion can inhibit ribonucleotide reductase (RR) activity that results in suppressed DNA synthesis. Importantly, Iron depletion induces hypoxia and consequently promotes the expression of HIF-1α. HIF-1α can initiate the transcription of genes involved in angiogenesis and iron uptake, namely, VEGF and TfR, respectively. Iron chelation can also result in elevated p53 protein levels via the HIF-1α. Increased p53 stability then results in G1/S arrest and apoptosis via downstream effectors including p21. Furthermore, HIF-1α mediates EMT by upregulating Snail and TWIST1 expression. Increased p53 also induce various EMT transcription factors including ZEB-1 and miR200, and these factors upregulate PD-L1 expression. Eribulin treatment improves tumor immune microenvironment such as hypoxia, EMT and immune check point induced by iron depletion.

Supplementary Files

This is a list of supplementary files associated with this preprint. Click to download.

- NC3RsARRIVEGuidelinesChecklistfillable.pdf